

## Dehydroxylation and structure of alumina gels prepared from trisecbutoxyaluminium

R.L. Frost\*, J. Kloprogge, S.C. Russell, J.L. Szetu

*Centre for Instrumental and Developmental Chemistry, Queensland University of Technology, 2 George Street, GPO Box 2434, Brisbane, Qld 4001, Australia*

Received 3 September 1998; received in revised form 3 December 1998; accepted 15 December 1998

---

### Abstract

The dehydroxylation of alumina gels prepared from the hydrolysis of trisecbutoxyaluminium has been studied using a combination of differential thermal analysis and infrared emission spectroscopy. Trisecbutoxyaluminium was hydrolysed in water at both 25°C and 90°C. The alumina phase in the gel was found by both DTA and FTIR absorption and FTIR emission spectroscopy to be gibbsite. The 25°C hydrolysed gel showed endotherms at 82°C, 168°C and 244°C which were attributed to the dehydration of adsorbed and surface coordinated water, and to the dehydroxylation of the gibbsite in the alumina gel. The weight loss in the first two endotherms was 23% and 10% showing that the gel had a high water content. The gel formed at 90°C shows endotherms at 62°C, 251°C, 277°C, 404°C and 538°C. The first endotherm was attributed to the loss of adsorbed water, the 251°C and 277°C endotherms to the dehydroxylation of the gibbsite and the endotherms at 404°C and 538°C to the dehydroxylation of boehmite in the gel. The structure and dehydroxylation of the gel was determined by both infrared absorption and emission spectroscopy. © 1999 Elsevier Science B.V. All rights reserved.

*Keywords:* Alumina; Bauxite; Gibbsite; Gel; Dehydroxylation; Infrared emission; FTIR; Trisecbutoxyaluminium

---

### 1. Introduction

The use of thermal techniques to study the dehydration and dehydroxylation of gibbsite and other  $\text{Al}_2\text{O}_3\text{-H}_2\text{O}$  minerals has been widely documented [1]. Little attention has been paid to alumina gels. It is clear that many variables must be taken into account when using techniques such as DTA, DSC, TGA, CRTA and quasi-isothermal TGA and isobaric TGA [2–6]. Such variables include heating rate, external pressure, water vapour pressure and even sample particle size [7]. The initial step in the thermal decomposition of gibbsite is the diffusion of protons and the

reaction with hydroxyl ions to form water [8–11]. This process removes the binding forces between the strata of the gibbsite structure and changes in the chemical composition and density within the layers. Published DTA patterns of a coarse-grained gibbsite show an endotherm centred on 230°C followed by a second at 280°C [11]. This latter endotherm is attributed to the formation of boehmite by hydrothermal conditions due to the retardation diffusion of water out of the larger grains. This endothermic reaction does not occur in the DTA patterns of finely grained gibbsite. A shallow endotherm may be observed between 500°C and 550°C and is attributed to the formation of boehmite. There is a general agreement that boehmite and a disordered transition alumina is formed

---

\*Corresponding author.

upon the thermal treatment of coarse gibbsite up to 400°C. When fine-grained gibbsite is heated rapidly, an X-ray amorphous product labelled  $\rho$ -alumina is obtained [12]. It is uncertain whether this phenomena was due to fine grain size or to the rapid heating.

The use of vibrational spectroscopy to study the phases of the  $\text{Al}_2\text{O}_3\text{--H}_2\text{O}$  system has been extensive over a long period of time [13]. Synthetic polycrystalline gibbsite showed bands at 3617, 3520, 3428 and 3380  $\text{cm}^{-1}$ . These bands were assigned to the hydroxyl-stretching frequencies. Bending vibrations were observed at 1020, 958 and 914  $\text{cm}^{-1}$ . Other bands were found at 802 and 743  $\text{cm}^{-1}$ . van der Marel and Beutelspacher [14] reported the infrared spectra of a large number of samples from the  $\text{Al}_2\text{O}_3\text{--H}_2\text{O}$  system including gibbsite (hydrargillite), boehmite, bayerite and nordstrandite. Bands were identified for gibbsite at 3620, 3520, 3450 and 3380  $\text{cm}^{-1}$  in the hydroxyl-stretching region. Bands were also found at 1100, 1020, 968, 940 and 915  $\text{cm}^{-1}$ . Two low frequency bands were observed in many of the samples at 836 and 745  $\text{cm}^{-1}$  [14]. Boehmite showed bands at 3297 and 3090  $\text{cm}^{-1}$  with bending vibrations at 1160 and 1080  $\text{cm}^{-1}$  [15]. Infrared absorption bands for diaspore were found at 2994 and 2915  $\text{cm}^{-1}$  for the hydroxyl-stretching frequencies and 1077  $\text{cm}^{-1}$  for the bending vibration and 963  $\text{cm}^{-1}$  for the hydroxyl deformation [16–18]. Infrared has been used to show the development of crystalline structure in aluminium polymorphs on ageing [18]. In this work, three high frequency bands were found at 3622, 3529 and 3460  $\text{cm}^{-1}$ , which showed progressive sharpening on ageing. Naumann et al. [6] suggested that infrared could be used to estimate the extent of the lattice defects in gibbsites. The application of infrared spectroscopy and its range of techniques have been widely used to study gibbsites [18,19]. However almost no research on the spectroscopy of alumina gels has been forthcoming.

Infrared emission spectroscopy allows the possibility of studying the dehydroxylation of minerals at elevated temperatures. The technique of measurement of discrete vibrational frequencies emitted by thermally excited molecules, known as Fourier transform infrared emission spectroscopy (FTIR ES) [20–22], has not been widely used for the study of mineral structures. The major advantages of IES are that the samples are measured in situ at *elevated temperatures*

and IES requires no sample treatment other than making the  $\text{Al}_2\text{O}_3\text{--H}_2\text{O}$  sample of submicron particle size. Further the technique removes the difficulties of heating the sample to dehydroxylation temperatures and quenching before measurement, as IES measures the dehydroxylation process as it actually takes place [23,24]. Here in this paper we report the study of the dehydroxylation of an alumina gel using the FTIR ES technique.

## 2. Experimental

### 2.1. Synthesis of alumina sols and gels

Alumina hydrolysates were prepared by the reaction of trisecbutoxyaluminium in both cold (25°C) and hot (90°C) water. The resulting precipitates were washed several times with water to remove the organic reaction products, namely alcohol, then diluted in water to give slurries with  $\text{Al}_2\text{O}_3$  concentrations such that the concentration of aluminium is  $\sim 0.6$  mol. Hydrolysate slurries were agitated by the use of a magnetic stirrer at room temperatures to prepare the sol. Nitric acid dispersing agent was added in a ratio of 0.1 mol  $\text{HNO}_3$  per mole of  $\text{Al}_2\text{O}_3$ . Samples of the sols produced were collected from the peptisation vessel and allowed to gel by solvent evaporation.

### 2.2. Thermal analysis

Differential thermal analysis of the crushed gels was obtained using a Setaram DTA/TGA instrument, operating at 0.5°C/min from ambient temperatures to 650°C.

### 2.3. Infrared emission spectroscopy

FTIR emission spectroscopy was carried out on a Digilab FTS-60A spectrometer, which was modified by replacing the IR source with an emission cell. A description of the cell and principles of the emission experiment have been published elsewhere [20–22]. Approximately 0.2 mg of size fractionated alumina gel (<0.5  $\mu\text{m}$  sample size) was spread as a thin layer on a 6 mm diameter platinum surface and held in an inert atmosphere within a *nitrogen purged* cell with an additional flow of argon over the sample during heating.

Detailed experimental spectroscopic procedures have been published [20–22]. In the normal course of events, three sets of spectra are obtained: firstly, the black body radiation over the temperature range selected at the various temperatures, secondly, the platinum plate radiation is obtained at the same temperatures, and thirdly, the spectra from the platinum plate covered with the alumina gel sample. Normally only one set of black body and platinum radiation is required.

The emittance spectrum at a particular temperature was calculated by subtraction of the single beam spectrum of the platinum backplate from that of the platinum+sample, and the result ratioed to the single beam spectrum of an approximate blackbody (graphite). This spectral manipulation is carried out after all the spectral data have been collected. The spectra of a series of alumina gels may be obtained and in the spectral manipulation, the same sets of black body and platinum hot plate radiation are used for all the gel spectra. The emission spectra were collected at intervals of 25°C, over the range 100–600°C. The time between scans (while the temperature was raised to the next hold point) was approximately 100 s. Scans were monitored until thermal equilibrium was obtained; this usually required approximately 3–5 min. The spectra were acquired by coaddition of 128 scans for temperatures 100–300°C (approximate scanning time 140 s) and 64 scans for temperatures 300–600°C (approximate scanning time 45 s), with a nominal resolution of  $\sim 4\text{ cm}^{-1}$ . Good quality spectra can be obtained provided the sample thickness is not too large. If too large a sample is used then the spectra become difficult to interpret because of the presence of combination and overtone bands. In fact the best quality spectra come from very thin samples of the alumina gel on the platinum plate.

The IES technique depends on the difference in temperature between the sample and the detector for its success. Thus the greater the difference between the sample temperature and the detector the better the quality of the spectrum in terms of signal to noise. Hence spectra at the lower temperatures always contain more noise. This means that the useful temperature range for the study of dehydroxylation is from 100°C and above. The difficulty of lack of signal for the low frequency region is not as pronounced. The OH stretching region is noisier because it is the high-energy region of the spectrum. As the temperature goes up more energy is available at higher wave numbers (Planck's law) therefore at any temperature (up to about 900°C) there is more energy at lower wave number, which gives a higher signal/noise ratio. It is for this reason that the signal gets better as the temperature is increased. Emittance values vary from 0 to 1 with a scale equivalent to an absorption spectrum. The data were linearised with respect to concentration where required by transforming to units of  $-\log 10(1-\text{emittance}(\nu))$ . Spectral manipulation such as baseline adjustment, smoothing and normalisation was performed using the Spectracalc software package (Galactic, Salem, NH, USA).

### 3. Results and discussion

#### 3.1. Differential thermal analysis

The differential thermal analysis of the two gels formed at 25°C and 90°C are shown in Fig. 1. The component peak fitting of the endotherm for the 90°C DTA pattern is shown in Fig. 2. Table 1 shows the results for the analysis of the two alumina gels, and

Table 1  
Endotherms and percentage areas of the endotherms of alumina gel, gibbsite and boehmite

Sample	Endotherm 1		Endotherm 2		Endotherm 3		Endotherm 4		Endotherm 5	
	<i>T</i> (°C)	Area (%)	<i>T</i> (°C)	Area (%)	<i>T</i> (°C)	Area (%)	<i>T</i> (°C)	Area (%)	<i>T</i> (°C)	Area (%)
Alumina gel (25°C)	82	71.5	168	13.5	244	15.0				
Alumina gel (90°C)	62	14.7	251	23.0	277	43.4	404	15.4	538	3.0
Gibbsite (synthetic)	223	3.9	261	27.2	284	62.4			301	5.6
Gibbsite (natural)					277	66	294	34		
Boehmite (synthetic)			486	43	500	57				
Boehmite (natural)	337	10	365	18	400	32.6	435	36		

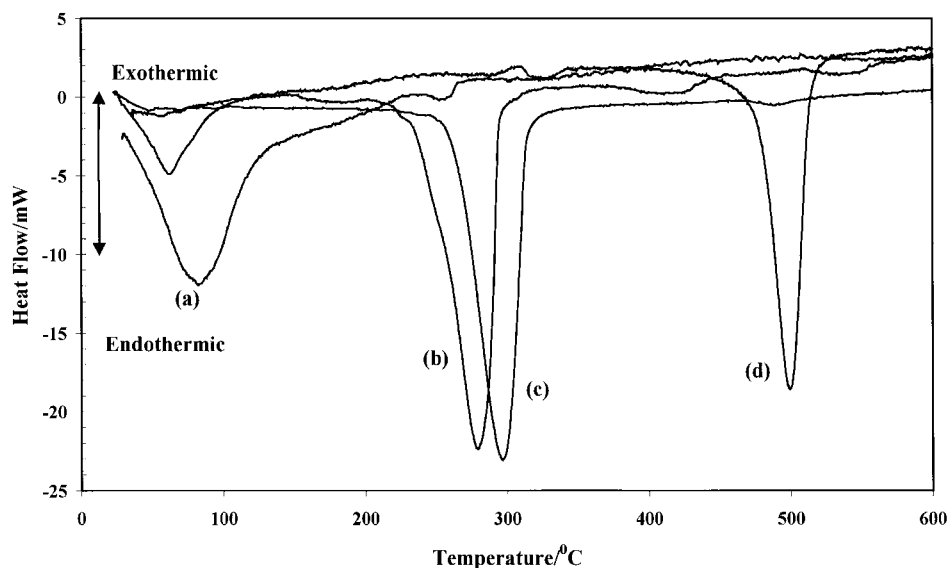


Fig. 1. Differential thermal analysis of alumina gels formed at (a) 25°C, (b) 90°C, (c) synthetic gibbsite and (d) boehmite.

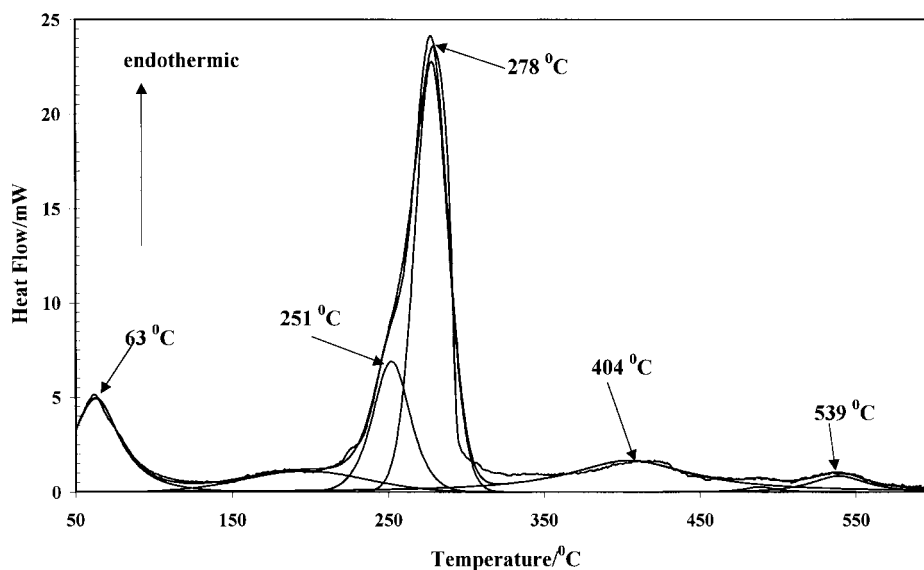


Fig. 2. Component peak analysis of the endotherms of the 90°C alumina gel.

synthetic and natural boehmites and gibbsites. The alumina gel formed at 25°C shows endotherms at 82°C, 168°C and 244°C. The areas of these endotherms are 71.5%, 13.5% and 15%, respectively. The weight losses for the three endotherms are 23%, 10% and 6.7%, respectively. The first two endotherms

are attributed to water in the alumina gel and the second to the dehydroxylation of the alumina phase. Synthetic boehmite shows two dehydroxylation endotherms at 486°C and 500°C. Synthetic gibbsite shows endotherms at 261°C and 284°C. Minor endotherms are also observed at 223°C and 301°C.

It is concluded that the endotherm at 244°C in the gel formed at 25°C is due to the dehydroxylation of gibbsite. This structure was confirmed by X-ray diffraction. The gel formed at 90°C shows endotherms at 62°C, 251°C, 277°C, 404°C and 538°C which have areas of 14.7%, 23.0%, 43.4%, 15.4% and 3%. It is concluded that the 90°C gel contains predominantly gibbsite with some boehmite. This assessment was confirmed by X-ray diffraction. The weight loss associated with the first endotherm is 5.7%. The weight loss for the 277°C endotherm is 21.3% and for the 404°C endotherm is 4.3%. Thus the ratio of gibbsite formation to boehmite is ~5:1.

### 3.2. Infrared emission spectroscopy

An important aspect of coating substrates with an alumina sol is the gel–ceramic transition. A suitable method of studying this transition is to use infrared emission spectroscopy. This technique enables the chemical and phase reactions of the gel–ceramic transition to be followed. Fig. 3 shows the spectra from 100°C to 650°C at 50°C intervals for the 90°C gel. The spectra are noisy because of the superimposition of water vapour bands on top of the alumina gel spectrum. The spectra are noisy at the lower tempera-

tures because of the low thermal energy. The spectra may be considered in sections according to the molecular vibration being studied. Thus the spectra may be considered in the (a) 3000–3500, (b) 1550–1650, (c) 1000–1100 and (d) 450–1000  $\text{cm}^{-1}$  regions. These regions may be attributed to the hydroxyl stretching, the water bending, the N–O symmetric stretching and the low frequency region.

Infrared absorption bands were identified in the alumina gels at 3620, 3520, 3450 and 3380  $\text{cm}^{-1}$  in the hydroxyl-stretching region. Bands were also found at 1100, 1020, 968, 940 and 915  $\text{cm}^{-1}$ . Table 2 reports a summary of the infrared absorption bands of synthetic and natural boehmites, gibbsites and diaspore. The close correspondence between the infrared absorption spectrum of the synthesised alumina gel and gibbsite confirms the alumina phase in the gel is gibbsite. Figs. 4 and 5 show the infrared emission spectra of gibbsite and boehmite, respectively. The broad bands which are in 3000–3700  $\text{cm}^{-1}$  region in Fig. 3 are attributed to the hydroxyl stretching of water in the alumina gels combined with the hydroxyl-stretching frequencies of the alumina phase. The results of the band component analysis of this hydroxyl-stretching region are reported in Table 3. In the 200°C spectrum, bands were identified at 3640, 3540,

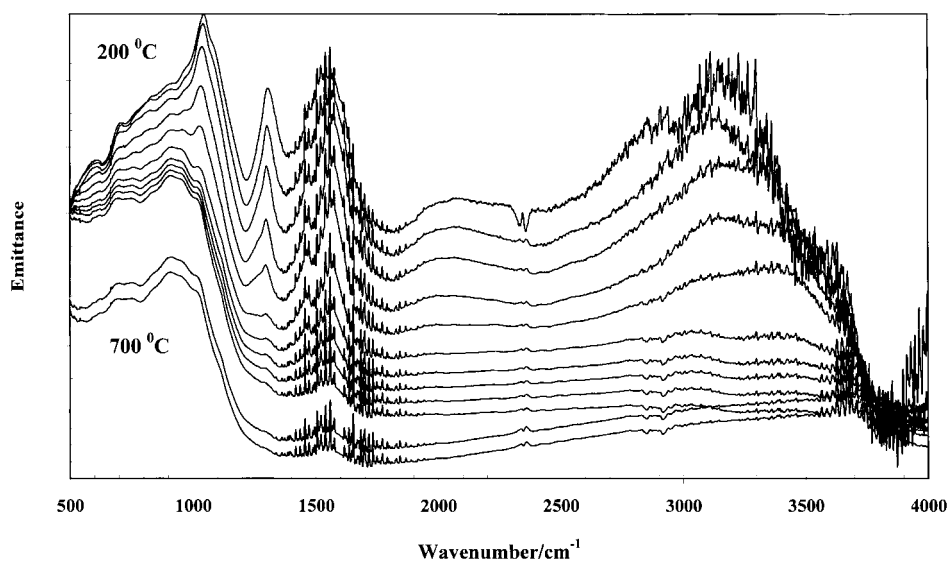


Fig. 3. Infrared emission spectra of alumina gel formed from the hydrolysis of trisecbutoxyaluminium(III) at 90°C and peptised with nitric acid.

Table 2

Structural data of the FTIR absorption bands of the hydroxyl-stretching and bending frequencies ( $\text{cm}^{-1}$ ) of gibbsite, boehmite and diaspore  $\nu(\text{AlO})$   $\delta(\text{Al-O})$   $\gamma(\text{AlO})$ 

Compound	$\nu(\text{OH})$				$\delta(\text{OH})$				$\gamma(\text{OH})$					
Diaspore				3365	3284	3095	2938	1151	1079					
Gibbsite (synthetic)	3660	3620	3525	3452	3394	3375	3338	1059	1023	969	938			
Gibbsite (natural)		3621	3526	3460	3436	3377	3285	1054	1020	967	942	915		
Boehmite (synthetic)			3413		3283	3096	2977	1152	1081	1036	1012	749	635	542
Boehmite (natural)			3430		3275	3092	2931	1135	1071	1034	1007	748	626	539

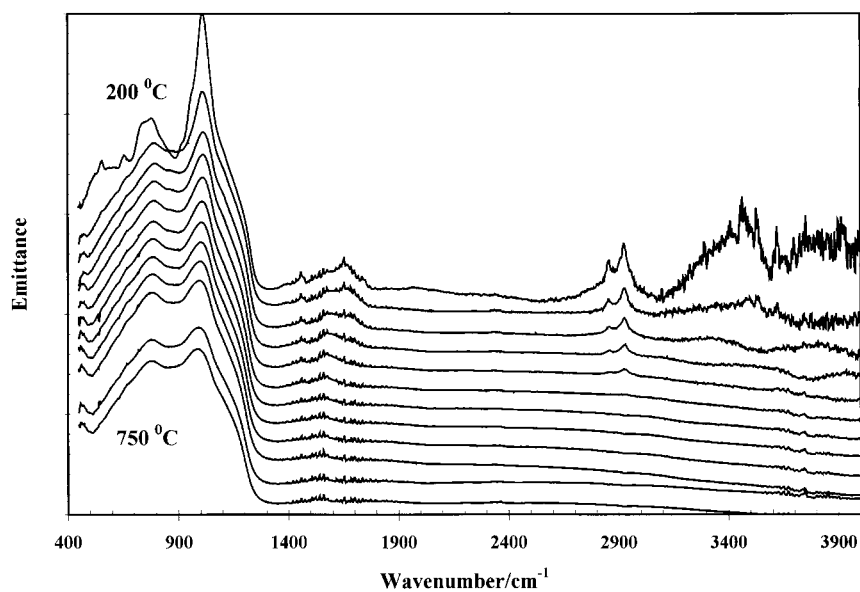


Fig. 4. Infrared emission spectra of synthetic gibbsite from 200°C to 750°C at 50°C intervals.

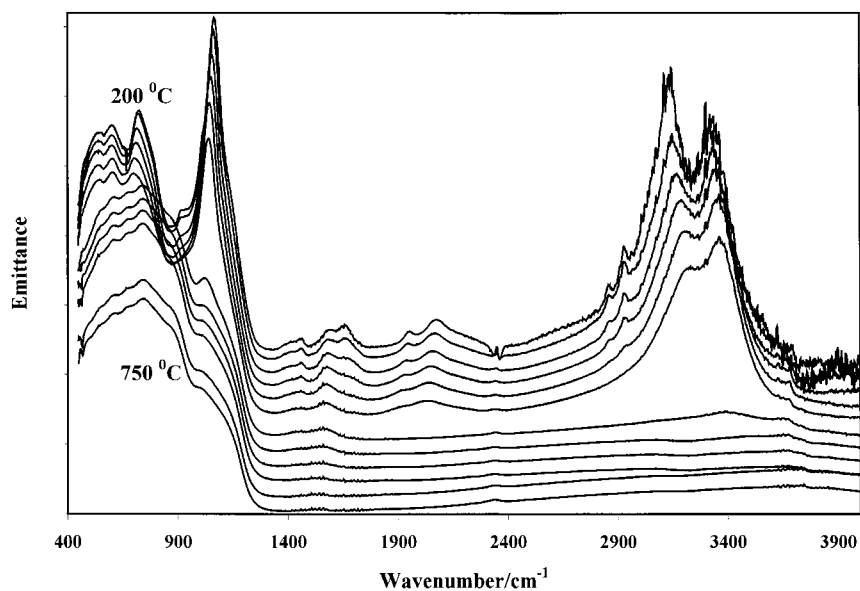


Fig. 5. Infrared emission spectra of synthetic boehmite from 200°C to 750°C at 50°C intervals.

3340 and 3109  $\text{cm}^{-1}$ . Fig. 6 shows the variation in band centres as a function of temperature. The 3640  $\text{cm}^{-1}$  band shows an increase in band position as the temperature is raised until 400°C where no intensity remains. Synthetic gibbsite also shows a

band in this position and so this band is assigned to an AlOH stretching vibration. The 3540  $\text{cm}^{-1}$  band also has an equivalent absorption band at 3525  $\text{cm}^{-1}$ .

Boehmite shows two sharp infrared emission bands at 3120 and 3340  $\text{cm}^{-1}$ . Gibbsite shows infrared

Table 3  
Band component analysis of the hydroxyl-stretching region of the 90°C alumina gel

Band	Temperature (°C)					
	200	250	300	350	400	450
Band centre (cm <sup>-1</sup> )	3640	3648	3655	3660	3664	3365
Intensity (%)	12.5	10.5	5.0	3.5	9.0	20.4
Band centre (cm <sup>-1</sup> )	3540	3535	3526	3523	3511	3517
Intensity (%)	6.6	7.3	6.3	10.3	7.7	3.9
Band centre (cm <sup>-1</sup> )	3340	3344	3363	3360	3380	3410
Intensity (%)	17.0	19.0	22.4	24.9	30.4	33.3
Band centre (cm <sup>-1</sup> )	3109	3106	3139	3120	3120	3058
Intensity (%)	65.0	63.0	66.0	61.0	52	42.4

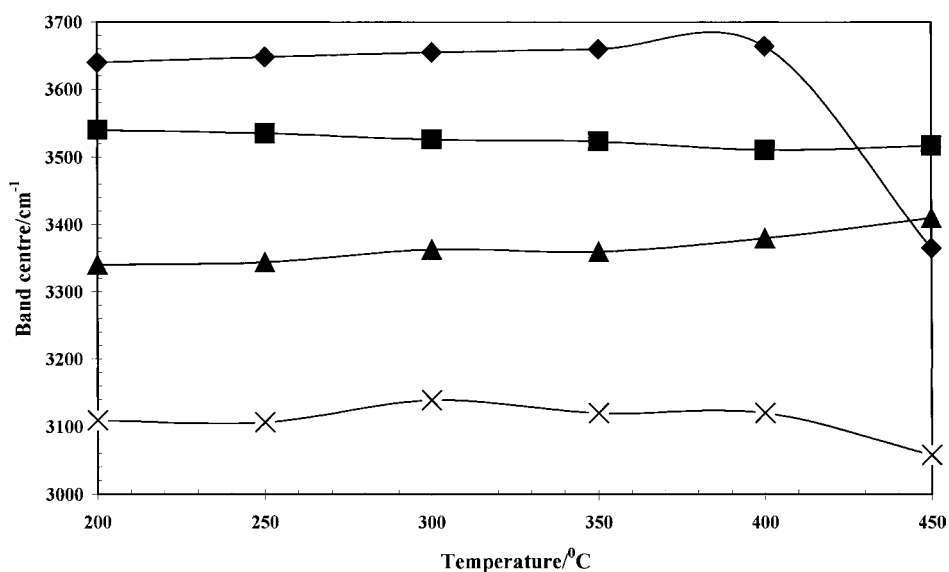


Fig. 6. Variation in the hydroxyl-stretching bands of thermally treated alumina gels as a function of temperature.

emission bands at 3132 and 3620 cm<sup>-1</sup>. It is unlikely that there are any hydroxyl-stretching frequencies attributable to other alumina phases. Thus the infrared emission spectra of the alumina gel should correspond to either gibbsite or boehmite or a combination of the two phases. In the IES spectra of the alumina gel, the spectral profile is broad with overlapping bands. The spectra show a distinct shift in band centre as the temperature is increased. The band at 3109 cm<sup>-1</sup> shifts to 3340 cm<sup>-1</sup> at 400°C. After this point no more water is lost. Thermal treatment of the water in the alumina gel causes the hydrogen bonding strength to be less thus resulting in an increase in the water

hydroxyl frequency. The water bending mode shows a single band at 1570 cm<sup>-1</sup>. This suggests water is loosely bound and is only weakly hydrogen bonded. These water molecules also show a hydroxyl-stretching band at 3550 cm<sup>-1</sup> in the absorption spectrum of the gel. Such a band is not observed in the IES spectra as the water has been lost before the first useful spectrum at 200°C is obtained.

The band centred at 1306 cm<sup>-1</sup> in the 200°C spectrum is attributed to the asymmetric stretching frequency of the N–O of the stabilising nitrate ion (Table 4). This band shows a strong shift to lower frequencies on heating. The band is centred at



Table 4

Results of the band component analysis of the low frequency region of alumina gel over the temperature range 200–600°C

Bands (cm <sup>-1</sup> )	Temperature (°C)								
	200	250	300	350	400	450	500	550	600
Band centre	1308	1306	1299	1293	1292	1296	1290		
	1055	1055	1052	1048	1043	1040	1038	1035	1032
	912	906	909	908	908	908	908	909	908
	801	787	785	785	789	789	790	791	790
	706	695	692	690	694	694	694	694	694
	584	587	572	561	563	563	564	575	575

1305 cm<sup>-1</sup> at 200°C and is at 1290 cm<sup>-1</sup> at 400°C. After this temperature, there is no significant intensity remaining. The band at 1045 cm<sup>-1</sup> is the infrared emission band of the nitrate N–O symmetric stretch. This band also shows a strong shift to lower frequencies on heating (see Table 4). The band is at 1028 cm<sup>-1</sup> at 450°C. It is proposed that this shift in band centre reflects the change in structure of the nitrate ion. At 200°C, the nitrate is simply a surface stabilising anion on the alumina surface. At 450°C, the nitrate is now a coordinated nitrate on the aluminium, i.e. it is a nitrate ligand. After this temperature little intensity remains in this band. It is significant that the spectrum of the low frequency region remains unchanged and is the infrared emission spectrum of

alumina. Natural gibbsite also has a hydroxyl bending vibration at the frequency of 1054 cm<sup>-1</sup>, which corresponds to the nitrate symmetric stretch. The mole ratio of nitrate to alumina is 0.1. Thus this band may therefore be attributed to the hydroxyl deformations in the alumina gels.

Low frequency bands are observed in the thermally treated gels. Bands are observed at 1306, 1055, 906, 787, 695 and 587 cm<sup>-1</sup> in the 250°C spectrum. The band at 1306 cm<sup>-1</sup> disappears after 500°C. The 1055 cm<sup>-1</sup> band shows a decrease in position with temperature and is observed at 1032 cm<sup>-1</sup> at 600°C. This band corresponds to a frequency observed in  $\alpha$ -alumina. However, the IES spectra of the heated gels do not correspond with that of corundum. The

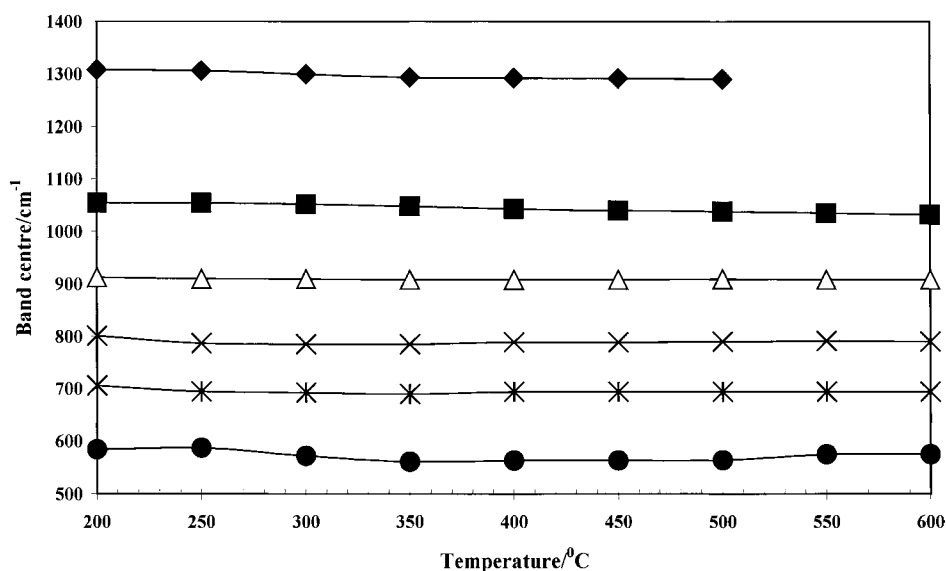


Fig. 7. Variation in the low frequency bands of thermally treated alumina gels as a function of temperature.

spectra more closely resemble that of  $\chi$ -alumina. Fig. 7 shows the variation of band position of the low frequency vibrations with temperature.

#### 4. Conclusions

The alumina gel formed from the acid peptisation of the hydrolysate formed from the reaction of trisecbutoxyaluminium(III) with water is shown to be gibbsite. Peptisation at 90°C resulted, additionally, in the formation of boehmite as determined by X-ray diffraction and infrared emission spectroscopy. The hydroxyl-stretching region is composed of overlapping bands from the gibbsite and boehmite. Low frequency bands of the thermally treated gel corresponded to the bands of  $\chi$ -alumina.

#### Acknowledgements

The Centre for Instrumental and Developmental Chemistry, Queensland University of Technology is gratefully acknowledged for financial support for this project. Prof. Graeme George is thanked for the use of the infrared emission spectrometer.

#### References

- [1] E. Lodding, The gibbsite dehydroxylation fork, in: R.F. Schwenker, P.D. Gran (Eds.), *Thermal Analysis*, vol. 2, Inorganic Materials and Physical Chemistry, Academic Press, New York, 1969, pp. 1239–1250.
- [2] J. Rouquerol, F. Rouquerol, Thermal decomposition of aluminium hydroxides, in: S.C. Beva, S.J. Gregg, N.D. Parkyn (Eds.), *Prog. Vacuum Microbalance Tech.*, Plenum Press, New York, 1973, 35 pp.
- [3] J. Rouquerol, F. Rouquerol, M. Ganteaume, Thermal decomposition of gibbsite under low pressures. Formation of the boehmite phase I, *J. Catal.* 36 (1975) 99–110.
- [4] J. Rouquerol, F. Rouquerol, M. Ganteaume, Thermal decomposition of gibbsite under low pressures. Formation of microporous alumina II, *J. Catal.* 57 (1979) 220–230.
- [5] F. Paulik, J. Paulik, R. Naumann, K. Kohnke, D. Petzold, Mechanism and kinetics of the dehydration of hydragillite. Part I, *Thermochim. Acta* 64 (1983) 1–14.
- [6] R. Naumann, K. Kohnke, J. Paulik, F. Paulik, Kinetics and mechanism of the dehydration of hydragillites. Part II, *Thermochim. Acta* 64 (1983) 14–24.
- [7] L. Candela, D.D. Perlmutter, Pore structures and kinetics of the thermal decomposition of  $\text{Al}(\text{OH})_3$ , *AICHe* 32 (1986) 1532.
- [8] W. Feitknecht, A. Wittenbach, W. Buser, Fourth Symposium on Reactivity of Solids, Elsevier, Amsterdam, 1961, pp. 234–239.
- [9] R. Freund, *Ber. Deut. Keram. Ges.* 42 (1965) 23.
- [10] R. Freund, *Ber. Deut. Keram. Ges.* 44 (1967) 141.
- [11] C. Colombo, A. Violante, The effect of time and temperature on the chemical composition and crystallisation of mixed iron and aluminium species, *Clays Clay Minerals* 44 (1967) 113.
- [12] V.J. Ingramjones, R.C.T. Slade, T.W. Davies, J.C. Southern, S. Salvador, Dehydroxylation sequences of gibbsite and boehmite – study of differences between soak and flash calcination and of particle-size effects, *J. Mater. Chem.* 6 (1996) 73.
- [13] V.C. Farmer, *Infrared spectra of minerals*, Mineralogical Society Monograph, vol. 4, Mineralogical Society, London, UK, 1974, pp. 149–151.
- [14] H.W. van der Marel, H. Beutelspacher, *Atlas of Infrared Spectroscopy of Clay Minerals and their Admixtures*, Elsevier, Amsterdam, 1976, pp. 224–229.
- [15] J.J. Fripiat, H. Bosmans, P.G. Rouxhet, Proton mobility in solids. 1. Hydrogenic vibration modes and proton delocalisation in boehmite, *J. Phys. Chem.* 71 (1967) 1097–1112.
- [16] V.A. Kolesova, Ya.I. Ryskin, Infrared spectra of diaspore, boehmite, and gallium oxyhydroxide, *Zh. Strukt. Khim.* 3 (1962) 680–684.
- [17] E. Schwarzmann, H. Sparr, Hydrogen bridge bonds in hydroxides with diaspore structure, *Z. Naturf. B* 24 (1969) 8.
- [18] H. Elderfield, J.D. Hem, The development of crystalline structure in aluminium hydroxide polymorphs on ageing, *Mineral. Mag.* 39 (1973) 89.
- [19] P.G. Smith, H.R. Watling, P. Crew, The effects of model organic compounds on gibbsite crystallisation from alkaline aluminate solutions – polyols., *Colloids Surfaces A* 111 (1996) 119.
- [20] A.M. Vassallo, P.A. Cole-Clarke, L.S.K. Pang, A. Palmisano, *J. Appl. Spectrosc.* 46 (1992) 73.
- [21] R.L. Frost, K. Finnie, B. Collins, A.M. Vassallo, Infrared emission spectroscopy of clay minerals and their thermal transformations, in: R.W. Fitzpatrick, G.J. Churchman, T. Eggleton (Eds.), *Proceedings of the 10th International Clay Conference*, CSIRO, Adelaide, Australia, 1995, pp. 219–224.
- [22] R.L. Frost, A.M. Vassallo, The dehydroxylation of the kaolinite clay minerals using infrared emission spectroscopy, *Clays Clay Minerals* 44 (1996) 635–651.
- [23] R.L. Frost, G.A. Cash, J.T. Klopogge, Rocky Mountain leather, sepiolite and attapulgitite – an infrared emission spectroscopic study, *Vibrational Spectrosc.* 16 (1998) 173.
- [24] J.T. Klopogge, R.L. Frost, The dehydroxylation of basic aluminium sulfate: an infrared emission spectroscopic study, *Thermochim. Acta* 320 (1998) 245.